Development of a generalized integral jet model

Duijm, Nijs Jan; Kessler, A.; Markert, Frank

Published in:
Proceedings of the 7th International Conference on Hydrogen Safety

Publication date:
2017

Document Version
Peer reviewed version

DEVELOPMENT OF A GENERALIZED INTEGRAL JET MODEL

Duijm, N.J.[1,2], Keßler A.[3] and Markert, F.[4]
[1] Dept. of Management Engineering, Technical University of Denmark DTU, Produktionstorvet 424, 2800 Kgs. Lyngby, Denmark, nidu@dtu.dk
[2] Nicestsolution, Baunegaardsvej 16, 4040 Jyllinge, Denmark, nicestsolution@duijm.dk
[3] Fraunhofer Institute for Chemical Technology, Joseph-von-Fraunhofer Str. 7, 76327 Pfinztal, Germany, armin.kessler@ict.fraunhofer.de
[4] Dept. of Civil Engineering, Technical University of Denmark DTU, Brovej 118, 2800 Kgs. Lyngby, Denmark, fram@byg.dtu.dk

ABSTRACT

Integral type models to describe stationary plumes and jets in cross-flows (wind) have been developed since about 1970. These models are widely used for risk analysis, to describe the consequences of many different scenarios. Alternatively, CFD codes are being applied, but computational requirements still limit the number of scenarios that can be dealt with using CFD only. The integral models, however, are not suited to handle transient releases, such as releases from pressurized equipment, where the initially high release rate decreases rapidly with time. Further, on gas ignition, a second model is needed to describe the rapid combustion of the flammable part of the plume (flash fire) and a third model has to be applied for the remaining jet fire. The objective of this paper is to describe the first steps of the development of an integral-type model describing the transient development and decay of a jet of flammable gas after a release from a pressure container. The intention is to transfer the stationary models to a fully transient model, capable to predict the maximum extension of short-duration, high pressure jets. The model development is supported by conducting a set of transient ignited and unignited spontaneous releases at initial pressures between 25bar and 400bar. These data forms the basis for the presented model development approach.

1.0 INTRODUCTION

Integral models are widely used in consequence assessment, but they lack capabilities with respect to transient releases, ignition, and obstacles. Integral models are not as detailed as CFD models, but give fast calculation results. Therefore, integral models can be routinely used to handle large numbers of accident scenarios.

Integral type models to describe stationary plumes and jets in cross-flows (wind) have been developed since about 1970 [1]. Similar models have been developed for stationary jet fires [2,3]. These models are the “back bone” of nowadays commercial hazard consequence assessment software, such as PHAST® (by DNV GL), and EFFECTS® (by TNO).

These models however, are not suited to handle transient releases, such as releases from pressurised equipment, where the initially high release rate decreases rapidly with time. When the gas ignites, a separate second model is needed to describe the rapid combustion of the flammable part of the plume (flash fire) and another third model for the remaining jet fire.

Estimating the maximum length of a release with an initial “puff” and decreasing release rate afterwards is an issue, especially for releases from high-pressure pipe networks, such as gas mains, where the outflow reduces quickly due to resistance in the piping. Reliable predictions requiring smaller uncertainty margins can save society for substantial costs.

The alternative to the use of “integral models” are fully 3-dimensional CFD (Computational Fluid Dynamics) models. These models are nowadays routinely used in risk analysis, but due to limitations in both computational effort and not least efforts needed to interpret the results, these models are used for a limited number of release scenarios, and we have not yet seen these models routinely applied on

transient release scenarios. CFD calculations for risk assessment cover typically some 10, at maximum up to 50 scenarios. This leads always to uncertainty whether worst case scenarios are adequately covered in the analysis or not.

In the following some first experimental results and theoretical considerations are discussed in the development of integral models describing transient behaviour.

1.1 Problem statement

Consequence assessment of releases of hydrogen and other pressurized gases needs models to describe the extent of the jets to the limits of the hazardous concentrations. Either simple correlations (for simple axisymmetric jets) or 1-dimensional integral models (for jets in a crossflow or with buoyancy) are used. These models describe stationary jets, and transient releases (because of pressure reduction in the vessel) usually are modelled by a sequence of semi-stationary jets. For releases with fast dynamics, it can be questioned whether this approach is always adequate.

Figure 1 summarizes the results of this study. We present this Figure in the introduction to show that the results indeed confirm that the use of semi-stationary jets is inadequate. Figure 1 shows (a) the predicted position of the front of the jet according to the stationary theory (based on the centerline velocity or a “top-hat” averaged jet velocity); (b) results from preliminary transient CFD calculations; and (c) results from experiments. It is clear from the graph that the stationary theory overpredicts the development of the jet. The front of the transient jet travels half the distance as compared to the travelled distance of a particle in a stationary jet. This not only means that it takes longer time to reach some down-stream distance, it also implies that part of the gas released has spread sideways, potentially leading to wider hazardous (flammable) contours than a calculation with a stationary jet model would predict. We will revert to Figure 1 and the results presented herein in the following sections.

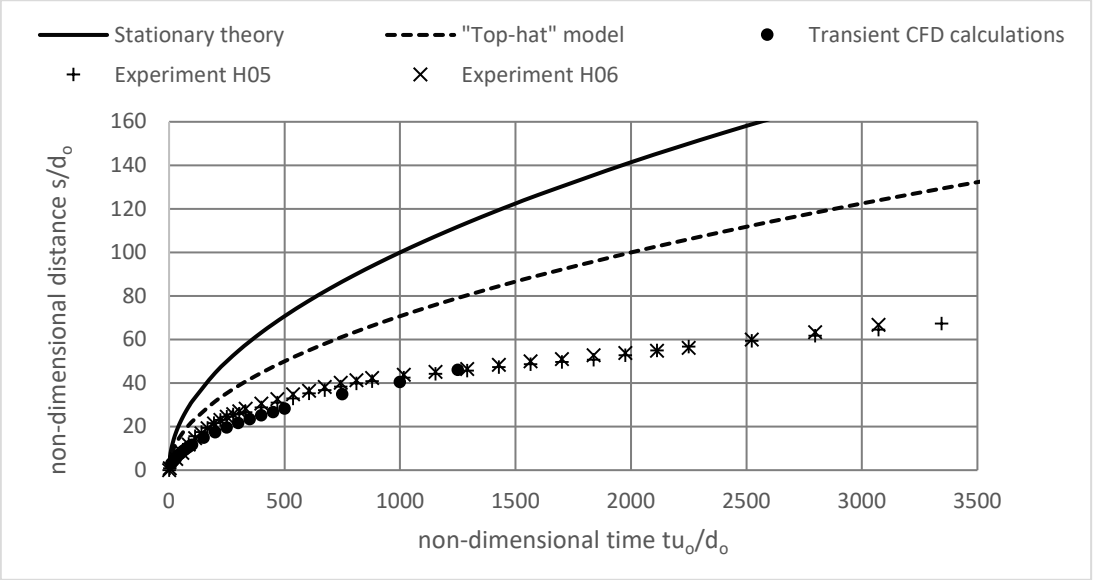

Figure 1 Comparison of the location of the front of a transient jet according to experiments and transient CFD calculations with the distance travelled in a stationary jet.

2.0 DEVELOPMENT OF A TRANSIENT INTEGRAL MODEL

2.1 The stationary one-dimensional jet

The model for the self-similar part of a free turbulent jet in a still fluid is based on a Gaussian distribution of velocity (the self-similar profile), where the radius is increasing linearly, and, as a consequence, the velocity decreases hyperbolically with downstream distance *s*. The formulae below are for the

incompressible case where the jet has the same density and thermodynamic properties as the fluid in which the jet is injected.

For the centerline velocity u_c one can write:

$$u_c(s) = \frac{u_0 \cdot d_0}{2 \cdot \sigma_u \cdot s} \qquad if \quad s > \frac{d_0}{2\sigma_u} \tag{1}$$

Where, $u_c(s)$ – centerline velocity, m/s; d_0 – source diameter, m; u_0 – initial velocity, m/s; σ_u – Gaussian deviation.

And for the radial distribution of velocity u:

$$u(y,s) = u_c(s) \cdot e^{-\left(\frac{y}{2 \cdot \sigma_u \cdot s}\right)^2} \tag{2}$$

Where, $u(y,s)$ – axial velocity, m/s; y – radial coordinate, m;.

The (dimensionless) standard deviation of the Gaussian profile is about 0.1 according to text books and the CFD calculations reported here [4,5].

The progress of the front of the jet s_f (or rather, the travelled distance of a particle in the jet) can be calculated by integrating velocity over time:

$$s_f(t) = \sqrt{\frac{u_0 \cdot d_0}{\sigma_u} \cdot t} \tag{3}$$

Defining dimensionless time as $t^* = t \cdot u_0/d_0$, this can be written as:

$$\frac{s_f}{d_0} = \sqrt{\frac{t^*}{\sigma_u}} \tag{4}$$

This distance is shown in Figure 1 under the legend “stationary theory”.

2.2 Development of a transient model

It is attempted to build on the existing one-dimensional or maximum gradient models for stationary jets and plumes. The theoretical background for stationary integral models for jets and plumes in the atmosphere is well-established. The models are based on the assumption that the trajectory ***s*** of the plume follows the streamline of velocity in the centre of the plume, i.e.: *dx/ds* is proportional to $u_x(s)/|u(s)|$; *dy/ds* is proportional to $u_y(s)/|u(s)|$, where *u(s)* is the velocity of the points on the plume axis, see Figure 2.

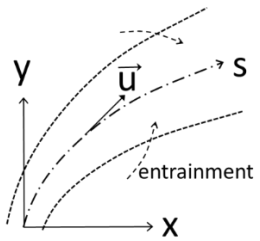

Figure 2 Principle of integral models

In this stationary, Eulerian approach, plume width and integral variables in the plume, such as momentum, total mass, pollutant mass, total enthalpy, etc., are one-dimensional functions of **s**, while the distribution of these (such as velocity, concentration) perpendicular to the plume axis are described

by similarity profiles as a function of plume width. The main process of interaction between the plume and its surroundings is through so-called "entrainment" of ambient air into the plume, where the entrained properties (ambient wind speed, ambient concentration and temperature) will change the integral variables in the plume [5]:

$$\frac{d(\dot{m}\cdot Q_j)}{ds} = E \cdot \rho_a \cdot Q_a \tag{5}$$

Where, $\dot{m}$ – total mass flow in the jet at a cross section at s [kg/s], Q – some property per unit mass; E – entrainment flow into the plume per unit length of the plume [m^2/s], ρ – density [kg/m^3]; index j refers to conditions in the jet, index a refers to the ambient conditions.

For $Q = 1$, this represents the mass balance in the jet, for $Q = u_x$ it represents the momentum balance in x-direction, etc. For some properties, additional terms may be of importance, e.g. buoyancy forces for the momentum in vertical direction, and terms representing pressure forces in case of crosswind. Entrainment is proportional to the local circumference of the jet, so it can be written as:

$$E = 2\,\pi r_j \cdot e \tag{6}$$

Where e is the "entrainment velocity". In the momentum-dominated region of the jet, the main driver for turbulent entrainment is the velocity difference between the jet and the ambient environment.

By using the parabolic nature of the flow, one can find the path $s(x,y,z)$ and the radius $R(s)$ of the stationary jet or plume by forward integration of the different balances for Q and the relations between mass flow and momentum. This model is an Eulerian description of the jet: we observe a fixed cross section at location s and consider the fluxes of mass and momentum passing that cross section, which is a suitable approach for stationary flows. For a transient model, a Lagrangian approach is more suitable, i.e. the jet is considered to exist of a series of connected "puffs". The formulas for the stationary jet or plume can be transformed to apply to a section of the jet, moving down stream. The governing formulas are then:

$$\frac{d(m\cdot Q_j)}{dt} = 2\,\pi R_j \cdot l \cdot e \cdot \rho_a \cdot Q_a \tag{7}$$

(m – mass in the "puff", R_j – radius of the puff and l – the length of the puff, all at time t).

The balances of momentum and mass can be integrated to get the size and path of each puff. However, we need additional relations to ensure that the collection of puffs remains a continuously linked jet. The Eulerian, stationary approach does not need to consider the interaction between parts of the jet along the axial dimension, but in case of transient behavior, where not all puffs have the same history, and therefore can go individual paths, the interaction between adjacent puffs need to be dealt with (the problem has become elliptic). When the puff at the front of the jet pushes against the air ahead, the drag force has to be distributed to the puffs behind. Similarly, when the release rate decreases, the later, slower puff has to remain attached and hold back the faster puff ahead.

Such connections can be provided by including pressure, albeit in a global, puff-averaged way. Pressure differences between the puffs' faces in axial direction add terms to the momentum balance for acceleration or deceleration. Pressure difference between the inside of the puff and the ambient environment controls the radial expansion or contraction of puffs needed to ensure continuity of the jet or plume so that adjacent puffs neither overlap nor have holes between them.

Dealing with pressure differences in axial direction seems a trivial exercise, as the net pressure difference becomes a term in the momentum balance for the movement of the center of the puff. Dealing with radial expansion using the "puff" framework is more challenging. It is not immediately obvious how the pressure difference between "inside" and "outside" can be defined, i.e. what is the proper selection for the circumferential area on which the pressure difference acts? Furthermore, radial

expansion (or compression) will generate resistance in the ambient flow-field, while the radial expansion, once set in motion, also represents momentum, in other words forces will be both functions of radial expansion (*dR/dt*) and changes of radial expansion (d^2R/dt^2). Therefore, we take a closer look into the radial expansion in the stationary jet.

For integral models, it is advantageous to consider bulk properties (of velocity, concentration, density) within the jet. This is equivalent to replacing the Gaussian profile by a "top hat" profile, i.e. a uniform value within a radius *R(s)* and zero (or the ambient value) outside. Equality of both momentum flow and volume flow between the top-hat profile and the Gaussian profile is obtained for a choice of the radius of:

$$\frac{R}{s} = 2\,\sigma_u \tag{8}$$

And the average velocity is half of the centerline velocity (index "b for "bulk"):

$$u_b(s) = \frac{u_c(s)}{2} \tag{9}$$

Figure 1 also shows the position of the front of the jet using this bulk velocity. Inserting these values in the expression for local entrainment, we obtain:

$$\frac{d\dot{V}}{ds} = (2\,\pi \cdot R\,) \cdot \left(\frac{\sigma_u}{2} \cdot u_c(s)\right) = (2\,\pi \cdot R\,) \cdot \left(\sigma_u \cdot u_b(s)\right) \tag{10}$$

So the entrainment velocity *e*, based on the reference radius *R*, amounts to $\sigma_u \cdot u_b$

Note that the growth of the radius is $\frac{dR}{ds} = 2\,\sigma_u$, but the entrainment velocity at radius *R* is only half of it. So the expansion of the jet is equally due to entrainment and to the deceleration of the jet (at a slower velocity, the diameter has to increase to allow the same volume to pass). The deceleration causes a radial velocity in the jet.

2.2 Preliminary CFD calculations

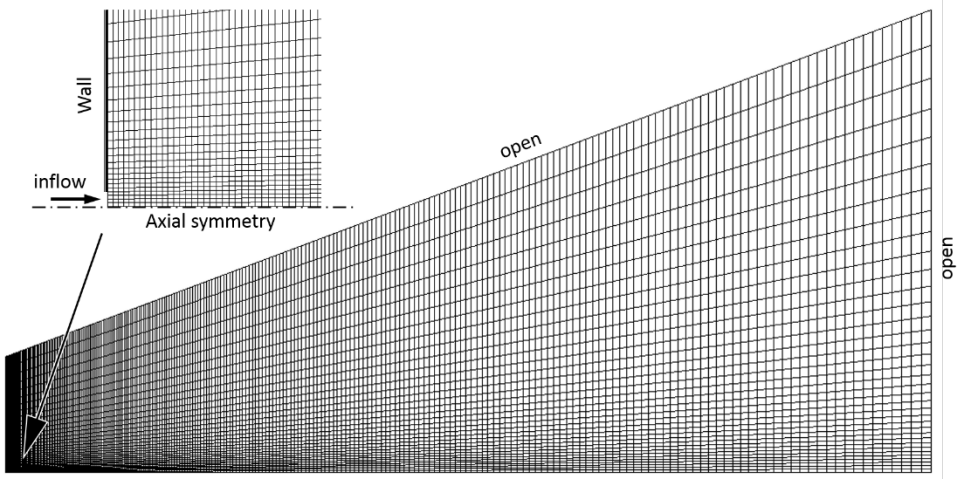

Figure 3 Domain and grid for the CFD calculations.

To obtain a better understanding of the processes in the radial direction, some CFD calculations where performed using OpenFoam with the standard k-ε model. Figure 3 shows the axial-symmetrical domain and grid. The calculations simulate a release from a hole of 10 mm diameter in a flat wall, with a release velocity of 10 m/s (so the Reynolds' number is about 6500). The length of the domain is 2 m, the radius

of the domain at the left-hand side is 0.3 m and at the right-hand side 1 m. The top-and right-hand side boundaries are open using an “atmosphere” boundary condition.

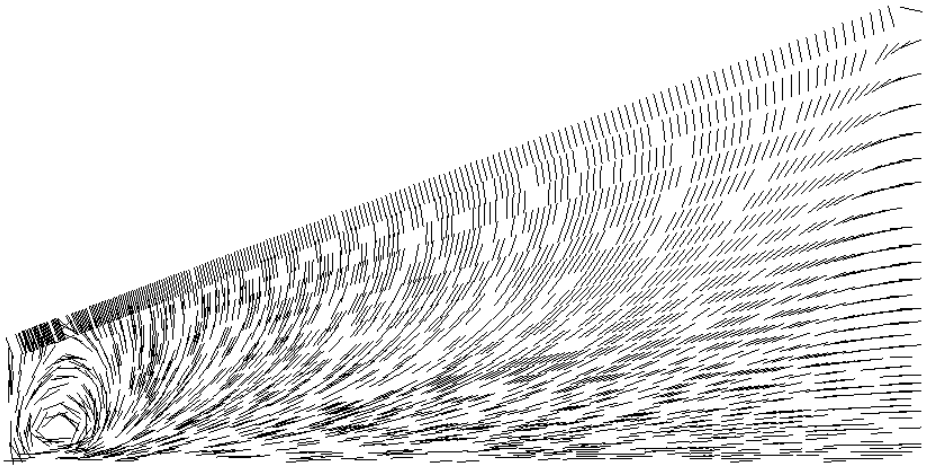

Figure 4 Flow direction at 0.2 s after start of the release.

Stationary and transient jets (using a step-change of release velocity at *t=0*) have been simulated. The front of the transient jet (the position where the velocity on the centerline is 50% of the velocity in the stationary solution) is shown in Figure 1. Figure 4 shows the flow direction in the transient calculation after 0.2 s.

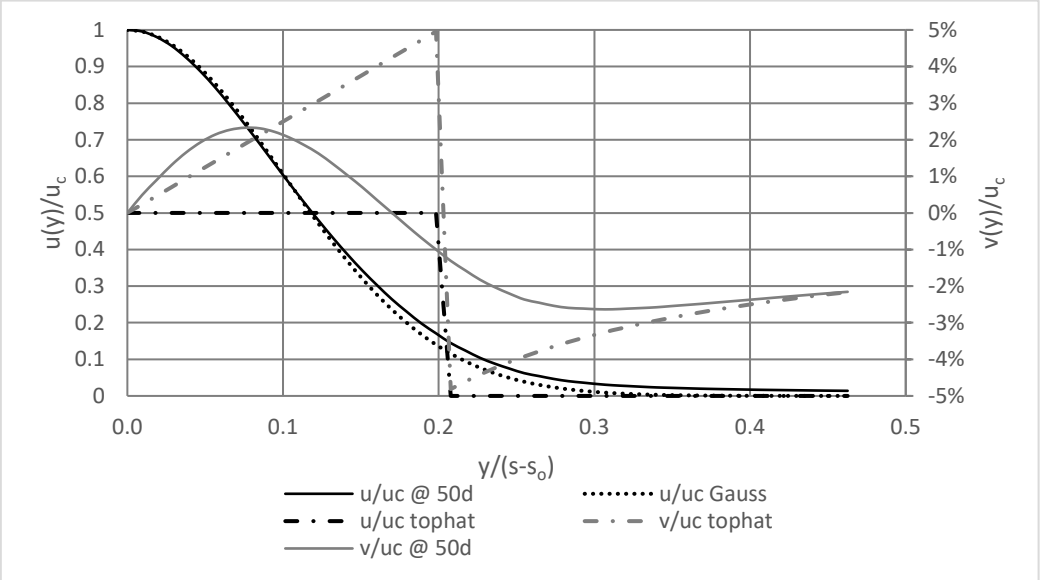

Figure 5 Dimensionless radial profiles of axial velocity (*u*, in black) and radial velocity (*v*, gray) at one downstream position (*s/d* = 50), scaled by the local axial velocity on the centerline from CFD simulation for the stationary condition as described for Figure 1. s_o is the displacement of the virtual jet point source of the similarity profiles as compared to the real release point. The Figure also shows the theoretical Gaussian axial velocity profile for σ_u = 0.1 and the” top-hat” profile with $R = 2\,\sigma_u$ and the radial velocity profile corresponding to the “top-hat” model (see text).

Figure 5 shows the radial profiles of axial velocity (*u*) and radial velocity (*v*) for the stationary CFD simulation. The axial velocity decelerates in the core, leading to an expansion and a positive, outward radial velocity with a maximum of about 2.5% of the centerline velocity. At the edges (*y/x* > 0.17), the axial velocity accelerates and the radial velocity is inward with a similar magnitude, this can be

conceived as the entrainment. This result agrees with the data presented in [6]. The Figure also shows the results for the "top-hat" model: in that case, the radial velocity in the jet would increase linearly to the edge of the jet to meet the expansion of the jet due to deceleration. Outside the jet (where the axial velocity component is zero), the fluid shall accelerate towards the jet inversely with distance to meet the entrainment velocity at the edge of the jet. Note the reasonable match of the radial velocity for the CFD results and the "top-hat" model for y/x > 0.4.

The radial velocity represents a momentum, i.e. it requires a force to set the fluid in radial motion. The force shall be some pressure difference between the center of the jet and the ambient condition. It seems an arbitrary choice only to consider the fluid inside the jet (in reality there is no sharp boundary), however that is what we do. In the puff with top-hat profile, the radial momentum is obtained by integrating

$$l \int_0^{2\pi} \int_0^{\mathrm{R}} v(r) r \, dr d\varphi \tag{11}$$

The general solution of this integral is:

$$\pi R l v(R) \tag{12}$$

$v(R)$ is the expansion velocity at the edge of the jet (the total growth of the jet is the sum of this expansion velocity and the entrainment velocity). Note that this integral represents momentum, not momentum flow. By using the relation between the change in puff length (axial compression) and radial expansion:

$$\pi \cdot R^2 \cdot \frac{dl}{dt} = -2\pi \cdot v(R) \cdot l \cdot R \tag{13}$$

We can express the momentum directly from the axial compression:

$$-\frac{\pi R^2}{2} \frac{dl}{dt} \tag{14}$$

The momentum per unit length of the jet of the stationary, self-similar (top-hat) jet can be shown to be:

$$\pi R l \sigma_u u_b \tag{15}$$

This is a constant function (u_b is inversely proportional with s and *R* is linear with *s*), so the momentum in the stationary jet does not change (except for the region close to the source where the jet has not established itself as a self-similar profile). This is in agreement with the observation from the stationary CFD calculations that there is no pressure gradient beyond the initial zone of jet establishment.

If we integrate the velocity profile obtained from the CFD calculations (see Figure 5), we find a radial momentum that is about 1/3rd of the value for the "top-hat" model.

2.3 Concept of the transient puff model

The concepts of the transient integral model are illustrated in Figure 6 showing a puff i connected to the earlier puff $i-1$ and the later puff $i+1$. The movement of the center of the puff is determined by (1) the initial momentum and the entrained fluid from the environment and (2) the net force from the differences in dynamic pressure on both sides of the puff. The velocity at the interface of the puff is the velocity of the center of the puff together with the relative movement of the interface due to the change in length of the puff, so the net dynamic force evaluated at the interfaces between the puffs of the puff *i* + 1 on puff *i* is:

$$\frac{\pi}{4}\left(\frac{R_i+R_{i+1}}{2}\right)^2 \left\{\left(v_{i+1} + \frac{1}{2}\frac{dl_{i+1}}{dt}\right) - \left(v_i - \frac{1}{2}\frac{dl_i}{dt}\right)\right\}^2 \tag{16}$$

It can be demonstrated that in a stationary condition, this net force will be zero and the static pressure inside the puff is the same as the ambient pressure, so the momentum of the radial expansion remains the same. In a transient condition, the dynamic pressure difference will have two effects: The resulting force in the direction of the jet will accelerate or decelerate the whole puff, and the cumulative difference from the end of the jet will change the radial expansion, thereby changing the terms *dl/dt*. The total movement of the transient jet is a result from the balance between changes in radial momentum and axial momentum. The description of this balance requires empirical input from experiments and CFD simulations.

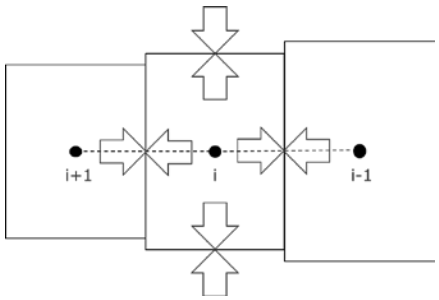

Figure 6 Model concept for the transient jet model. Three puffs interact by pressure and adjustment of radial expansion to remain connect.

3.0 EXPERIMENTAL SETUP

The experimental set-up to generate turbulent transient jets was established at the open air experimental plant building of Fraunhofer ICT. The set-up and facility is shown in Figure 7 and Figure 8. It consists of gas supply system with a pressure reservoir of a volume of ~5 l, which was able to store hydrogen at pressures up to 400bar and a concrete wall as background for the jet investigation.

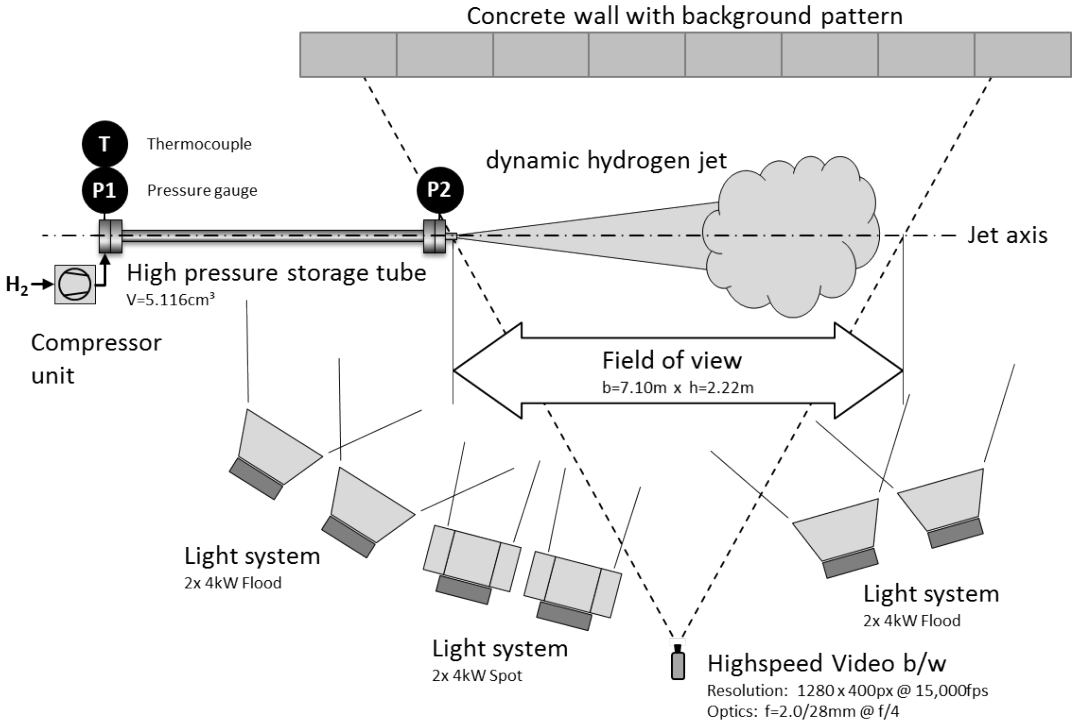

Figure 7 Experimental set-up at Fraunhofer ICT.

Figure 8 Open air experimental plant building of Fraunhofer ICT to be used for the high pressure storage tube (l.) and the concrete wall, here with an ignited jet in front of it (r.)

The release section of the high-pressure storage tube is shown in Figure 9. It shows the conical reduction of the 40.3 mm storage tube to the horizontally oriented 10 mm dia. release pipe. This release pipe has an effective length of 101 mm, represents the restriction orifice and limits hydrogen mass flow out of the high-pressure storage tube.

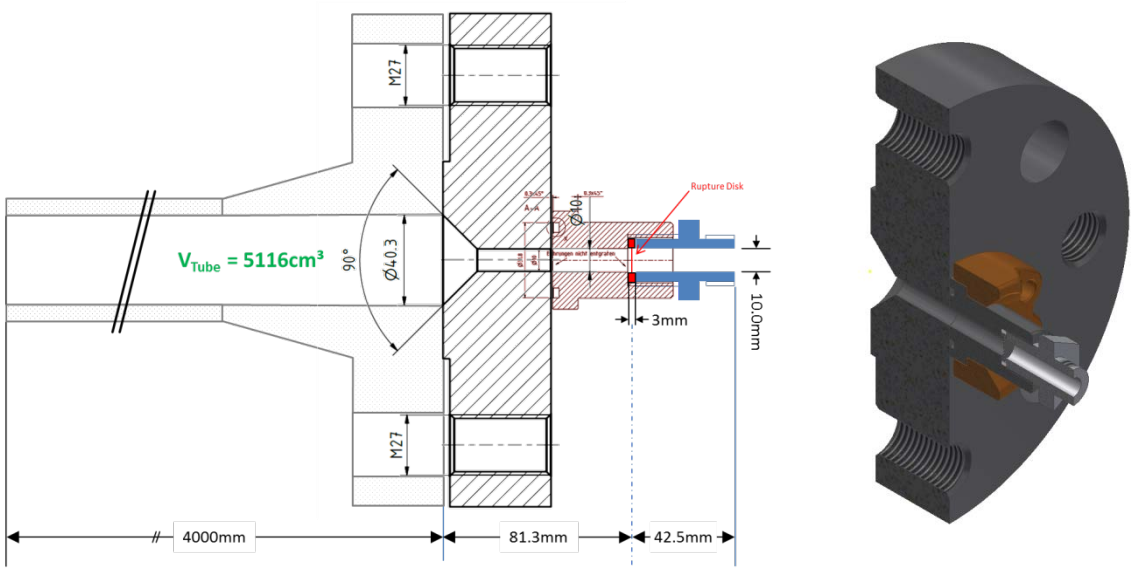

Figure 9: Schematic (l.) and rendered (r.) cross cut of the release section with conical reduction to 10mm dia. of the release pipe where the rupture disk is inserted.

A rupture disc holder was constructed within the release pipe to avoid shock pressure induced auto ignition. The rupture disk holder houses so-called manometer screw-connection rupture disks. This type of rupture disks was selected due to its availability in a broad pressure range with identical dimensions. It ensures opening of the whole release pipe cross section without further restrictions at low activation pressure scattering of ±10 %.

Despite the intended suppression of auto ignition in every second pre-test instantaneous ignition of the jet occurred during the putting in operation phase. Sliding spark ignition was identified as reason for this effect. It is caused by statistical rupture disk splinter impact to the inner surface of the downstream part inside the release pipe. This unintended ignition could be suppressed by combination of two countermeasures: The inner surface of the release pipe was moistened using soap water and the release orifice was additionally closed using a thin foil tape strip and inertised with nitrogen using a syringe.

The setup is fully remote controlled and generates well-defined highly dynamic jets which propagate horizontally into the field of view of the measurement equipment. The rupture disks were activated by pressure increase until they fail and the pressurized hydrogen relaxes into the free air. This spontaneous depressurisation induces downstream the rupture disk a shock wave and the subsequent hydrogen jet and upstream a dilution wave passing the high pressure storage tube. This dilution wave oscillates during the whole release process between both ends of the high pressure storage tube and appear on the pressure decay curves shown in Figure 10.

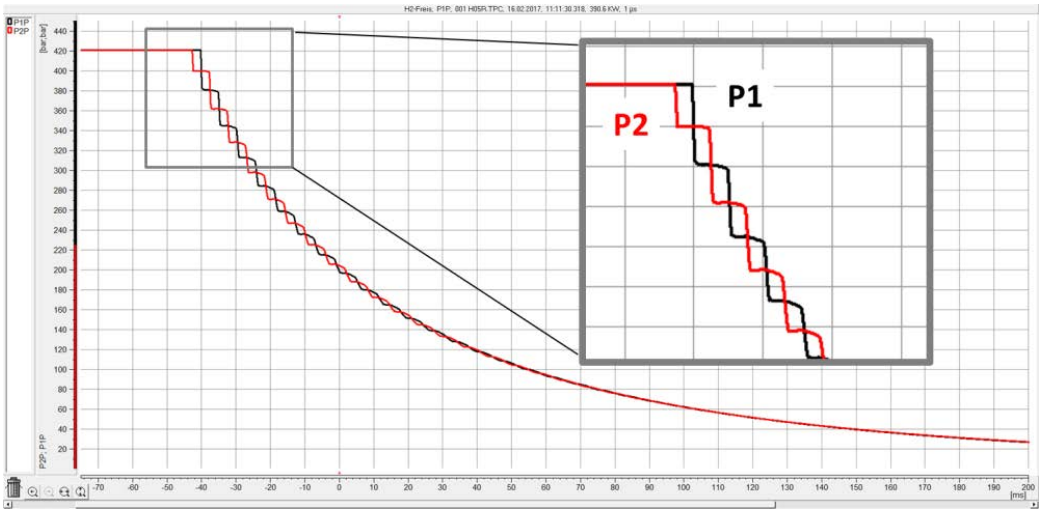

Figure 10: Pressure decay curves inside the high-pressure storage tube for sensor P1 in black color at the upstream end of the tube and sensor P2 in red color at the downstream end of the tube close to the reduction to the release pipe.

4.0 RESULTS

In total 20 experiments were carried out at initial pressures ranging from 25bar to 400bar in four pressure steps with and without ignition and two experiments for each case for reproducibility purposes.

Table 1. Measured release conditions

Nominal pressure [bar]	Activation pressure [bar]	t90-10 [s]	Initial pressure decay [bar/s]	Averaged pressure decay [bar/s]	Initial gas temperature [°C]
25	28.2 ±0.9	0.225 ±.000	310.9 ±10	95.2 ±3	12.8 ±0.1
100	105.6 ±2.9	0.218 ±.000	1350 ±37	376 ±10	12.3 ±0.3
200	222.6 ±5.8	0.200 ±.004	3206 ±97	837 ±25	11.4 ±0.4
400	409.2 ±12.1	0.180 ±.003	6739 ±233	1703 ±62	9.1 ±1.2

Pressure decay rates correlate to the rupture-disk activation pressure and decay exponentially. The related release conditions are given in Table 1 and are calculated from the acquired transient pressure transducer data during release. Initial pressure decay is the maximum value reached at the very beginning of the release; the averaged pressure decay is taken in the time $t_{90\text{-}10}$ which represents the decay time between 90% and 10% of the activation pressure.

Highspeed video acquisition was performed using the subframe capability of the Phantom V710 highspeed camera. Acquisition speed could be increased to 15,000fps at reduced resolution of 1280 x 400px. As background for the video analysis a mechanically stable modular concrete wall was applied.

This wall was painted in white colour and stamped with an irregular black dot pattern to allow high speed video analysis of both, ignited and unignited jets under identical conditions. Together with an in total 24kW light system exposure times for the single frame of 7µs could be realized.

The frames were evaluated with various techniques of image processing especially needed as pure hydrogen jets are nearly invisible in the visual spectral range. The BOS method uses a standard method of image processing [7] the cross correlation of neighboured images. It was proposed by the DLR Göttingen to the application to fluid dynamics [8,9] and introduced to hydrogen research by Fraunhofer ICT [10,11]. This procedure makes very small effects in fluids visible, which are generated by fluctuations in densities.

In this paper we present the preliminary analysis for two selected unignited 400bar experiments. The initial pressure and temperature have been converted into a flowrate, and for this condition the notional nozzle diameter and jet velocity have been calculated in order to be able to compare the results with the theory for incompressible flows [12,13], see Table 1. The brightness difference method was used to evaluate the jet front propagation on the jet axis.The notional nozzle and velocity have been used to define the dimensionless time- and distance scale and the results are included in Figure 1.

Table 2. Flow rate and notional properties calculated from release conditions for selected experiments.

Experiment	Activation pressure (bar)	Initial flow rate (kg/s)	Initial gas temperature (K)	Notional nozzle diameter (mm)	Notional jet velocity (m/s)
H05	421.52	1.602	282.19	105.2	2161
H06	421.41	1.583	283.01	105.5	2158

5.0 DISCUSSION AND CONCLUSIONS

The objective of the project is to develop an integral-type model describing the path and spreading of flammable gases in the environment. The model will be able to predict the development and path of jets and plumes from transient releases (such as decaying releases from pressurized equipment).

The concept for this transient model is based on the existing integral type models for stationary releases, transformed in a Lagrangian framework of connected “puffs”. In order to describe the interaction of the adjacent puffs, the differences in dynamic pressure will be used to balance between the acceleration or deceleration of the whole puff and the radial expansion of the puff. Experimental data and results from CFD simulations will be necessary to quantify the empirical parameters that govern this balance

The introduction of “pressure” in this way allows for future expansions of the model, viz.:

- A better description (as compared to existing stationary integral models) of the interaction of the jet or plume with obstacles such as walls, pipes and process vessels.

- The transient behaviour on ignition from an un-ignited plume through flash fire to a jet fire, viz the model would provide a generalized framework capable of describing un-ignited jets; ignited jets (jet flames); and the transition on ignition, i.e. a flash fire.

The main application of such model is in the field of risk analysis of installations handling hazardous materials, such as offshore installations, process industry, and installations in a hydrogen-fuelled transport infrastructure.

6.0 REFERENCES

1. Ooms G., Duijm N.J., Dispersion of a stack plume heavier than air, IUTAM Symposium "Atmospheric Dispersion of Heavy Gases and Small Particles." The Hague: Springer-Verlag, 1983.
2. Servert J., Crespo A., Hernandez J., A one-dimensional model of a turbulent jet diffusion flame in an ambient atmospheric flow, derived from a three-dimensional model, *Combust. Sci. Technol.* **124**, 1–6, 1997, pp. 83–114.
3. Duijm N.J., Jet flame attack on vessels, *J. Loss Prev. Process Ind.*, **7**, 2, 1994, pp. 161–166.
4. Rodi W. Turbulent Buoyant Jets and Plumes, HMT series, 1982, Pergamon Press, Oxford.
5. Ball C.G.G,, Fellouah H., Pollard A., The flow field in turbulent round free jets, *Prog. Aerosp. Sci.*, **50**, 2012, pp. 1–20.
6. Abraham J., Entrainment characteristics of transient gas jets, *Numer. Heat Transf. Part A Appl.*, **30**, 4, 1996, pp. 347–364.
7. Russ JC. The Image Processing Handbook, 1992, CRC Press, Boca Raton, FL.
8. Raffel M., Richard H., Meier G.E., On the applicability of Background Oriented Optical Tomography, *Exp. Fluids*., 2000, pp. 447–481.
9. Richard H., Raffel M., Rein M., Kompenhans J., Meier G.E.A., Demonstration of the applicability of a Background Oriented Schlieren (BOS) method, 10th Symposium of Applications Laser Techniques to Fluid, 2000.
10. Keßler A., Ehrhardt W., Langer G., Hydrogen detection: Visualisation of Hydrogen Using Non Invasive Optical Schlieren Technique BOS, 1st Int Conf on Hydrogen Safety, Pisa, Italy, 2005.
11. Blanc A., Deimling L., Eisenreich N., Langer G., Keßler A., Evaluation of optical and spectroscopic experiments of hydrogen jet fires, 3rd Int. Conf. Hydrogen Safety, Ajaccio, France, 2009.
12. Birch A.D., Hughes D.J., Swaffield F., Velocity Decay of High Pressure Jets, *Combust. Sci. Technol*., **52**, 1987, pp. 161–171.
13. Papanikolaou E., Baraldi D., Kuznetsov M., Venetsanos A., Evaluation of notional nozzle approaches for CFD simulations of free-shear under-expanded hydrogen jets, *Int. J. Hydrogen Energy*, **37**, 23, 2012, pp. 18563–18574.